NASA/TM–2016-219353

NASA AVOSS Fast-Time Models for Aircraft Wake Prediction: User's Guide (APA3.8 and TDP2.1)

Nash'at N. Ahmad and Randal L. VanValkenburg
Langley Research Center, Hampton, Virginia

Matthew J. Pruis
NorthWest Research Associates, Redmond, Washington

Fanny M. Limon Duparcmeur
Craig Technologies, Hampton, Virginia

November 2016

NASA STI Program . . . in Profile

Since its founding, NASA has been dedicated to the advancement of aeronautics and space science. The NASA scientific and technical information (STI) program plays a key part in helping NASA maintain this important role.

The NASA STI program operates under the auspices of the Agency Chief Information Officer. It collects, organizes, provides for archiving, and disseminates NASA's STI. The NASA STI program provides access to the NTRS Registered and its public interface, the NASA Technical Reports Server, thus providing one of the largest collections of aeronautical and space science STI in the world. Results are published in both non-NASA channels and by NASA in the NASA STI Report Series, which includes the following report types:

- TECHNICAL PUBLICATION. Reports of completed research or a major significant phase of research that present the results of NASA Programs and include extensive data or theoretical analysis. Includes compilations of significant scientific and technical data and information deemed to be of continuing reference value. NASA counter-part of peer-reviewed formal professional papers but has less stringent limitations on manuscript length and extent of graphic presentations.

- TECHNICAL MEMORANDUM. Scientific and technical findings that are preliminary or of specialized interest, e.g., quick release reports, working papers, and bibliographies that contain minimal annotation. Does not contain extensive analysis.

- CONTRACTOR REPORT. Scientific and technical findings by NASA-sponsored contractors and grantees.

- CONFERENCE PUBLICATION. Collected papers from scientific and technical conferences, symposia, seminars, or other meetings sponsored or co-sponsored by NASA.

- SPECIAL PUBLICATION. Scientific, technical, or historical information from NASA programs, projects, and missions, often concerned with subjects having substantial public interest.

- TECHNICAL TRANSLATION. English-language translations of foreign scientific and technical material pertinent to NASA's mission.

Specialized services also include organizing and publishing research results, distributing specialized research announcements and feeds, providing information desk and personal search support, and enabling data exchange services.

For more information about the NASA STI program, see the following:

- Access the NASA STI program home page at http://www.sti.nasa.gov

- E-mail your question to help@sti.nasa.gov

- Phone the NASA STI Information Desk at 757-864-9658

- Write to:
  NASA STI Information Desk
  Mail Stop 148
  NASA Langley Research Center
  Hampton, VA 23681-2199

NASA/TM–2016-219353

NASA AVOSS Fast-Time Models for Aircraft Wake Prediction: User's Guide (APA3.8 and TDP2.1)

Nash'at N. Ahmad and Randal L. VanValkenburg
Langley Research Center, Hampton, Virginia

Matthew J. Pruis
NorthWest Research Associates, Redmond, Washington

Fanny M. Limon Duparcmeur
Craig Technologies, Hampton, Virginia

National Aeronautics and
Space Administration

Langley Research Center
Hampton, Virginia 23681-2199

November 2016

Available from:

NASA STI Program / Mail Stop 148
NASA Langley Research Center
Hampton, VA 23681-2199
Fax: 757-864-6500

Contents

List of Acronyms, Abbreviations, and Symbols

AFR	Autonomous Flight Rules
AGL	Above Ground Level
APA	AVOSS Prediction Algorithm
ATM	Air Traffic Management
ATPG	Atmospheric Turbulence Profile Generator
ASOS	Automated Surface Observations System
AVOSS	Aircraft VOrtex Spacing System
AWAS	AVOSS Winds Analysis System
CW	Continuous Wave Lidar
DEN	Denver International Airport
DFW	Dallas/Fort Worth International Airport
EDR	Eddy Dissipation Rate (m^2/s^3)
EGPWS	Enhanced Ground Proximity Warning System
FAA	Federal Aviation Administration
IGE	In-Ground Effect
IM	Interval Management
Lidar	LIght Detection And Ranging
mae	mean absolute error
MEM	Memphis International Airport, Memphis, Tennessee
NAS	National Airspace System
NASA	National Aeronautics and Space Administration
NTSB	National Transportation Safety Board
NGE	Near-Ground Effect
OGE	Out-of-Ground Effect
PL	Pulsed Lidar
RASS	Radio Acoustic Sounding System
rmse	root mean square error
SAO	Surface Aerodrome Observations
SAPA	Simplified Aircraft Based Paired Approach
TASS	Terminal Area Simulation System
TDP	TASS Driven algorithms for wake Prediction
b_0	Initial vortex pair separation (m)
b_G	Wingspan of the wake vortex generator (m)
Γ_0	Initial vortex circulation (m^2/s)
Γ^*	Non-dimensional vortex circulation (normalized by Γ_0)
ρ	Air density (kg/m^3)
θ	Potential Temperature/Theta (K)
t^*	Non-dimensional time
t_0	Time taken for the vortex pair to descend a distance equal to b_0
V_G	Airspeed of the wake vortex generator (m/s)
V_0	Initial vortex pair descent velocity (m/s)
W_G	Weight of the wake vortex generator (kg)
y_0	Initial position of the vortex pair with respect to the runway centerline (m)
y^*	Non-dimensional lateral vortex position (normalized by b_0)
z_0	Initial vortex height AGL (m)
z^*	Non-dimensional vortex height (normalized by b_0)

Introduction

The National Aeronautics and Space Administration (NASA) has been developing fast-time wake transport and decay models to provide solutions for safe, efficient, and capacity-enhancing spacing standards for the National Airspace System (NAS). These models are empirical algorithms used for predictions of wake transport and decay based on aircraft parameters and ambient weather conditions. The aircraft dependent parameters include the initial vortex descent velocity and the initial vortex pair separation distance. The atmospheric initial conditions include vertical profiles of temperature or potential temperature, eddy dissipation rate (EDR), crosswind, and headwind. The model output consists of a time history of circulation strength and position for the port and starboard vortices. The wake models can be used for the systems level design of advanced air traffic management (ATM) concepts. It is also envisioned that at some later stage of maturity, these models could be used operationally, not only within the terminal airspace but also as onboard tools to support concepts such as dynamic separation of aircraft.

NASA's first fast-time wake transport and decay model was developed by Greene (1986). In the late 1990s, under NASA's Aircraft Vortex Spacing System (AVOSS) project, significant advances were made in wake vortex modeling based on the data from field experiments and large eddy simulations. The initial versions of the AVOSS Wake Vortex Prediction Algorithm (APA) were developed during the AVOSS program (Hinton 2001). The APA model computes the out-of-ground-effect (OGE) decay and descent based on Sarpkaya (Sarpkaya et al. 2001). The model has an algorithm for enhanced rate of decay during the ground effect developed by Proctor et al. (2000). The in-ground-effect (IGE) transport accounts for vortex spreading and rebound. The code development of the early versions of APA is described in Robins and Delisi (2002). The latest version of the APA model (Version 3.8) has several improvements which include: 1) better parameterization of atmospheric stratification based on laboratory studies, 2) improvements in the modeling of countersign vorticity, and 3) improved modeling of vortex rebound in the presence of the crosswinds. These improvements are described in detail by Delisi et al. (2016).

NASA has also developed the TASS (Terminal Area Simulation System) Derived Algorithms for Wake Prediction (TDP) model. In the TDP model, the Sarpkaya component is replaced with algorithms developed from parametric studies using large eddy simulations. The TDP model is described in Proctor et al. (2006) and Proctor (2009). The current version of the TDP model includes the effects of the crosswind shear gradient on transport (Proctor and Ahmad 2011). The mechanics of the IGE model are the same as in APA Version 3.4 which follow an approach similar to Corjon and Poinsot (1996) and Robins et al. (2002). TDP transitions into near-ground effect (NGE) at a non-dimensional height of $z^*= 1$ while APA's transition is at $z^*= 1.5$. Even with identical IGE modules (which is no longer the case given the improvements made in APA3.8), the model predictions of the TDP and APA in NGE/IGE can be different since they do not enter the NGE phase with the same decay rate and their bounding decay rates are also different in the IGE phase.

The wake models have been used in the past for forensic reconstruction of wake encounter related accidents by NASA (Proctor et al. 2004; Gloudemans et al. 2016), and by the National Transportation Safety Board (NTSB) (O'Callaghan 2013). Other applications have included safety analysis for new ATM concepts such as the Simplified Aircraft Based Paired Approach (SAPA). SAPA has been proposed for closely spaced parallel runways (Johnson, et al. 2013; Guerreiro et al. 2010). The fast-time models may also be used for dynamic self-separation in advanced ATM concepts such as Interval Management (IM) (Barmore et al. 2014) and Autonomous Flight Rules (AFR) (Wing and Cotton 2011).

The current distribution includes the latest versions of the APA (3.8) and the TDP (2.1) models. This User's Guide provides detailed information on the model inputs, file formats, and model outputs. A brief description of the Memphis 1995, Dallas/Fort Worth 1997, and the Denver 2003 wake vortex datasets is given along with the evaluation of models. A detailed bibliography is provided which includes publications on model development, wake field experiment descriptions, and applications of the fast-time wake vortex models.

Software Distribution

NASA's AVOSS Fast-Time Wake Prediction software distribution is given below:

```
avoss/
|
`--bin/
|   |
|   +-- apa38.exe
|   |
|   `-- tdp21.exe
|
`--doc/
|   `-- APA-UsersGuide.pdf
|
`--etc/
|   `-- cases.i, apa.nml
|
`--mem95/                  Memphis 1995 Wake Vortex Dataset
|   |
|   +-- ADATA/             aircraft information and initial vortex location
|   |
|   +-- QDATA/             vertical profiles of eddy dissipation rate
|   |
|   +-- TDATA/             vertical profiles of potential temperature
|   |
|   +-- UDATA/             vertical profiles of crosswinds
|   |
|   +-- UPROXY/            vertical profiles of proxy crosswinds
|   |
|   +-- VDATA/             vertical profiles of headwinds
|   |
|   +-- CWP/               Lidar data for port vortex
|   |
|   `-- CWS/               Lidar data for starboard vortex
|
`--dfw97/                  Dallas/Fort Worth 1997 Wake Vortex Dataset
|
`--den03/                  Denver 2003 Wake Vortex Dataset
|
`--run/
    |
    +-- apa.nml                        namelist file
    |
    +-- cases.i                        list of cases to run
    |
    +-- 1995-08-10-230029.apa38        APA3.8 output
    |
    `-- 1995-08-10-230029.tdp21        TDP2.1 output
```

The directory structure for the Dallas/Fort Worth and Denver datasets (not shown above) is similar to that of the Memphis dataset. Pulsed Lidar (PL) was deployed in Denver whereas a Continuous Wave Lidar (CW) was used in both the Memphis 1995 and Dallas/Fort Worth 1997 deployments. Headwinds and proxy crosswinds are not available in the Denver 2003 dataset.

Model Input/Output Filename Convention

The file names are chosen to give a unique identifier for each case and model run. The unique identifier has the following form:

YYYY_MO_DY_HRMNSC

where,

YYYY	=	Four digit year
MO	=	Two digit month
DY	=	Two digit day
HRMNSC	=	Six digit HourMinuteSeconds

Example:

Case **'2003_09_19_181019'** has the following associated input files:

2003_09_19_181019.ADATA	Initial Vortex Location & Aircraft Parameters
2003_09_19_181019.TDATA	Vertical Profile of Potential Temperature
2003_09_19_181019.UDATA	Vertical Profile of Crosswind
2003_09_19_181019.VDATA	Vertical Profile of Headwind (if available)
2003_09_19_181019.QDATA	Vertical Profile of Eddy Dissipation Rate

The model output is written to (depending on the model used):

2003_09_19_181019.apa38	APA3.8 output
2003_09_19_181019.tdp21	TDP2.1 output

Model Input File Formats

Several changes have been introduced in the file formats to account for modifications in the latest version of the APA model. APA3.8 has the ability to use headwinds (if available). The glide slope and the wake generator airspeed are inputs in the aircraft parameters input file. In the IGE phase, APA3.8 takes into account the effect of landuse category on wake decay. Currently, parameters have been defined for only two landuse categories (trees and grass). While these modifications were made to APA3.8 only, and not to TDP2.1, both APA3.8 and TDP2.1 use the same format for their input files.

An additional input file **`apa.nml`** is also required to run the models. Input file formats are described in detail in this section.

Namelist File (apa.nml)

The namelist file sets some of the I/O parameters. The model type is needed for post-processing tools only (default is set to **`apa38`**). The Lidar type can be defined as either continuous wave or pulsed. This option is also used by post-processing and visualization tools only (the default value is **`CW`**).

Since TDP2.1 does not use headwinds and there might be cases in which headwinds may not be available, the availability/usage of headwinds needs to be specified in the namelist file (the default for the parameter **`headwinds`** is set to **`false`**).

The models will generate Tecplot® files containing the environmental profiles of crosswind, headwind, eddy dissipation rate, and potential temperature if **`env_profiles`** is set to **`true`** (default value is **`false`**).

The wake vortex trajectory and circulation decay output is written in non-dimensional form if **`nondim_output`** is set to **`true`** (the default value is **`false`**).

The namelist parameters **`headwinds`**, **`env_profiles`**, and **`nondim_output`** are used by the wake models.

NAMELIST FILE (apa.nml)

```
! ----------------------------------------------------------------------
! - namelist file for apa/tdp code
! ----------------------------------------------------------------------

&namelist_input

 model_type = “apa38”         ! apa38; tdp21

 lidar_type = “CW”,           ! CW=Continuous Wave and PL=Pulsed Lidar

 headwinds = .false.,         ! headwinds usage

 env_profiles = .false.,      ! environmental profiles output

 nondim_output = .false.,     ! non-dimensional output

/

! ----------------------------------------------------------------------
! - end of namelist file
! ----------------------------------------------------------------------
```

Case Input File (cases.i)

The first seven lines list the paths to input data. Line number 8 has the total number of cases (maximum number of cases = 5000) in the file. Please note that the models do not read or use the Lidar data. The rest of the file lists the unique identifiers for each case. The path names should have a maximum length of 132 characters.

CASE FILE (cases.i)

```
/home/nnahmad/apa-models/data/MEM1995/ADATA/
/home/nnahmad/apa-models/data/MEM1995/QDATA/
/home/nnahmad/apa-models/data/MEM1995/TDATA/
/home/nnahmad/apa-models/data/MEM1995/UDATA/
/home/nnahmad/apa-models/data/MEM1995/VDATA/
/home/nnahmad/apa-models/data/MEM1995/CWP/
/home/nnahmad/apa-models/data/MEM1995/CWS/
20     !  total number of cases to run
1995-08-06-230412
1995-08-06-232159
.
.
and so on.....
```

Aircraft Parameters Input File (YYYY_MO_DY_HRMNSC.ADATA)

The first line in the file contains a count of the number of header lines that follow. The file shown in the example below has 11 lines of header information. After the header lines, the file contains the initial vortex location and the aircraft data: Initial lateral location of the vortex (y_0), initial height of the vortex (z_0), initial descent velocity (V_0), the separation distance (b_0) of the vortex pair, the airspeed of the vortex generator, glide slope, and the landuse factor used in the IGE phase. The last three inputs (airspeed, glide slope, and the landuse) are not used by the TDP model. MKS units are used for all parameters.

AIRCRAFT PARAMETERS FILE (YYYY_MO_DY_HRMNSC.ADATA)

```
11
# Location: MEM, 18L_TANG
# Run Number: 1026
# A/C Type: AT43
# Wing span* (m): 24.6
# Weight* (kg): 13940
# ACspeed* (m/s): 63.4
# Air Density* (kg/m3): 1.2
# This file was created on 22-Mar-2012 12:42:37 Pacific Time
# File created by Matt Pruis, NWRA, matt@nwra.com
# *If data not provided with original data set, then default values used.
# Data File Format: yo(m),zo(m),Vo(m/s), bo(m), ACspeed(m/s), gslope(deg), gefac
5.2895, 90.03, 0.76635, 19.321, 63.4, 3, 0.3
```

Potential Temperature Profile (YYYY_MO_DY_HRMNSC.TDATA)

The first line in the file contains a count of the number of header lines that follow. The file shown in the example below has 11 lines of header information.

The first line after the header information gives the total number of data points in the file. If negative, then the file contains potential temperatures, otherwise the data are temperatures. The rest of the file has two columns: the first column lists the AGL height in meters and the second column lists the potential temperature in K or temperature in °C. If the user inputs a temperature profile, then it is converted by the model to potential temperature (θ). The fast-time wake models use potential temperature in model calculations.

Please note that the latest version of APA (Version 3.8) requires potential temperature data as the input. Temperature profile, if provided, is not converted to potential temperature in APA3.8. The user must provide a potential temperature profile for APA3.8.

At least three data points are required in the initial profile and the points should extend above and below the heights of vortex descent trajectory. If the input potential temperature profile contains regions of unstable stratification, then those values are set to zero (neutral stratification) within both the APA and TDP codes.

Please make sure that in the environmental data profiles the first data point is for height **`z=0`**. Even if the simulations are for the en route applications, it is important to ensure that the first point of environmental data correspond to **`z=0`**.

Observations from various field sensors as well as simulation data from mesoscale models (Ahmad et al. 2013) can be used to generate the vertical potential temperature profiles.

POTENTIAL TEMPERATURE PROFILE DATA (YYYY_MO_DY_HRMNSC.TDATA)

```
11
# Location: MEM, 18L_TANG
# Run Number: 1026
# A/C Type: AT43
# Potential modifications from original data include:
# (1) extrapolation above and below profile (with N=0 in these regions)
# (2) removal of unstable regions that are not attached to ground
#     (with N=0 in these regions)
# This file was created on 22-Mar-2012 12:42:37 Pacific Time
# File created by Matt Pruis, NWRA, matt@nwra.com
# Data File Format (1st line): number of points
# Data File Format (remainder of file): z (m)  potential temperature (K)
-120
0, 303.98
5, 303.98
10, 304.04       and so on.....
```

Crosswind Profile (YYYY_MO_DY_HRMNSC.UDATA)

The first line in the file contains a count of the number of header lines that follow. The file shown in the example below has 5 lines of header information. The first line after the header information gives the total number of data points in the file. Heights are in meters and the crosswinds are in m/s. Crosswind profiles can be generated from the Lidar data or estimated from the wake vortex trajectory (Pruis et al. 2011). Simulation data from mesoscale models can also be used to generate the vertical crosswind profiles. Please make sure that in the crosswind data profiles the first data point is for height **`z=0`**. Even if the simulations are for the en route applications, it is important to ensure that the first point of environmental data correspond to **`z=0`**.

CROSSWIND PROFILE DATA (YYYY_MO_DY_HRMNSC.UDATA)

```
5
# Location: MEM, 18L_TANG
# Run Number: 1026
# A/C Type: AT43
# Data File Format (1st line): number of data points
# Data File Format (remainder of file): z (m)  Crosswind (m/s)
120
0, 2.124
10, 2.074
20, 2.382
30, 3.519       and so on.....
```

Headwind Profile (YYYY_MO_DY_HRMNSC.VDATA)

Similar in format to the crosswind file, but contains headwind (m/s). Heights are in meters. Headwinds, if available, are used by APA3.8. The earlier versions of APA and the current version of the TDP model (Version 2.1) do not use headwinds. Please make sure that in the headwind profiles the first data point is for height **`z=0`**. Even if the simulations are for the en route applications, it is important to ensure that the first point of environmental data correspond to **`z=0`**.

HEADWIND PROFILE DATA (YYYY_MO_DY_HRMNSC.VDATA)

```
5
# Location: MEM, 18L_TANG
# Run Number: 1026
# A/C Type: AT43
# Data File Format (1st line): number of data points
# Data File Format (remainder of file): z (m)  Headwind (m/s)
120
0, 1.124
10, 0.23
20, 0.54
30, 0.43       and so on.....
```

Eddy Dissipation Rate Profile (YYYY_MO_DY_HRMNSC.QDATA)

The first line in the file contains a count of the number of header lines that follow. The file shown in the example below has 5 lines of header information.

The first line after the header information gives the total number of data points in the file. The file shown in the example below has 100 points in the vertical profile. The rest of the file has two columns: the first column lists the AGL heights in meters and the second column lists the eddy dissipation rates in m^2/s^3.

Given observations of EDR at two different heights, the vertical EDR profile can be generated using atmospheric boundary layer similarity theory (Han et al. 2000). EDR profiles can also be estimated from Lidar data (Pruis et al. 2013). Input EDR values less than $10^{-7} m^2/s^3$ are set to $10^{-7} m^2/s^3$ within the models.

Please make sure that in the environmental data profiles the first data point is for height **`z=0`**. Even if the simulations are for the en route applications, it is important to ensure that the first point of environmental data correspond to **`z=0`**.

EDDY DISSIPATION RATE DATA (YYYY_MO_DY_HRMNSC.QDATA)

```
5
# Location: MEM, 18L_TANG
# Run Number: 1026
# A/C Type: AT43
# Data File Format (1st line): number of data points
# Data File Format (remainder of file): z (m)  EDR (m2/s3)
100
0, 0.0026156
5, 0.0026156
10, 0.0025098
15, 0.002405    and so on.....
```

Lidar Data File Format

Lidar Data File (YYYY_MO_DY_HRMNSC.CWP)

For each case there are two Lidar data files: one each for the port and the starboard vortices. The filename conventions are as follows:

2003_09_19_181019.CWP	Continuous Wave Lidar Port Vortex Data
2003_09_19_181019.CWS	Continuous Wave Lidar Starboard Vortex Data
2003_09_19_181019.PLP	Pulsed Lidar Port Vortex Data
2003_09_19_181019.PLS	Pulsed Lidar Starboard Vortex Data

In most of the field experiments only one type of Lidar was used and therefore a particular dataset will have either CW or PL files. In the Denver 2003 Field Experiment (Dougherty et al. 2004) both CW and PL Lidars were deployed.

The first line in the file contains a count of the number of header lines that follow. The file shown in the example below has 4 lines of header information. The first line after the header information gives the total number of data points in the file. The file shown in the example below has 21 data points in the wake trajectory. The first column in the file is the time followed by the location (lateral and vertical) and the circulation strength. Missing data points in the files are marked by a `-9999`. Please note that it is not uncommon for the Lidar files to contain points that include valid times and vortex positions, but for which the circulation cannot be calculated due to missing or invalid data values. Consequently for a given vortex, the plots of circulation may display fewer discrete points than do the corresponding plots of lateral transport or altitude.

LIDAR DATA FILE (YYYY_MO_DY_HRMNSC.CWP)

```
4
# Location: MEM, 18L_TANG
# Run Number: 1026
# A/C Type: AT43
# Data File Format: time_p(s), y_pos_p(m), z_pos_p(m), Circ_p(m2/s)
21
8.88, 5, 87, 125.9091
13.6, 18.4, 92.5, -9999
15.57, 20.5, 83.2, 123.7773   and so on.....
```

Estimation of the initial circulation from the Lidar data is challenging. It has not been fully determined what the Lidar is measuring during the rollup process. Until the rollup is complete the Lidar is not measuring the true circulation of the fully rolled-up vortex system behind the aircraft and may include the vorticity associated with the flap vortex. In the Lidar track file the time history begins as soon as the aircraft passes the Lidar scan plane. The models do not take into account the roll-up process and begin with the assumption of a fully rolled-up vortex pair at the time of initialization. Therefore, in the aircraft data file (ADATA files) theoretical values of V_0 and b_0 are used with the assumption of a fully rolled-up vortex pair. This can result in differences between Γ_0 in the Lidar file and Γ_0 ($= 2\pi V_0 b_0$) obtained from the ADATA file. Lidar data from three different wake experiments along with initial circulation estimates from the ADATA file are shown in Figure 1. It can be seen that the discrepancy between the Lidar data and the Γ_0 obtained from ADATA file in some cases can be very large.

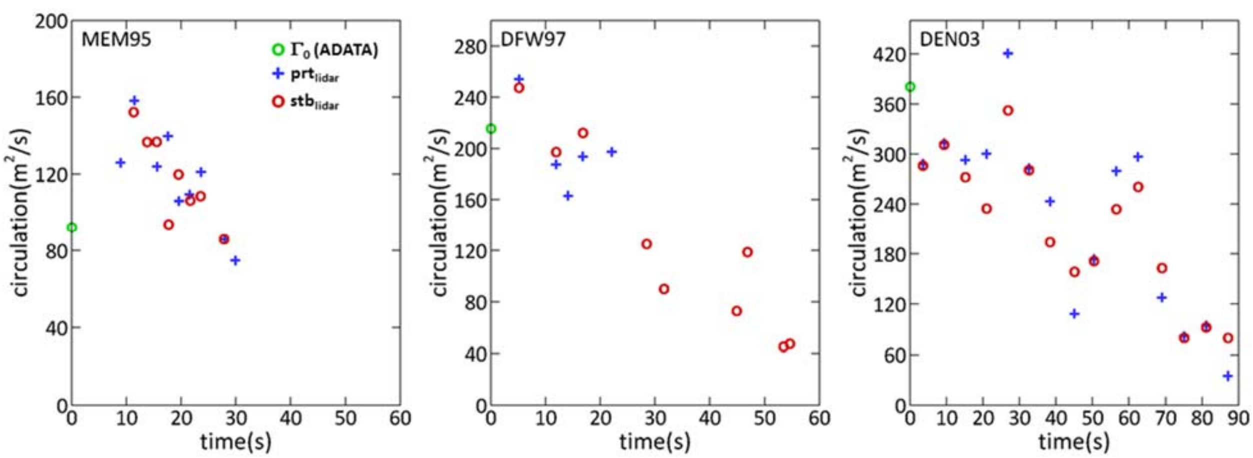

Figure 1: Comparison of Lidar data and Γ_0 obtained from the ADATA file for sample cases from MEM95 (left), DFW97 (center), and DEN03 (right) wake datasets. The Γ_0 obtained from the ADATA file is shown by the green circle.

Model Output File Format

Model Output File Format (e.g., YYYY_MO_DY_HRMNSC.apa38)

The model output file gives the time history of position (lateral distance and altitude) and circulation strength of both the port and starboard vortices. The output variables are listed in Table 1.

Table 1: Fast-Time Wake Model Output

Column #	Variable	Description
1	time	Time (seconds)
2	Yp	Lateral position of port vortex (m)
3	Zp	Altitude of port vortex (m)
4	Gp	Circulation of port vortex (m^2/s)
5	Ys	Lateral position of starboard vortex (m)
6	Zs	Altitude of starboard vortex (m)
7	Gs	Circulation of starboard vortex (m^2/s)

The output filename extension is based on the model type:

`2003_09_19_181019.apa38` APA3.8 output

`2003_09_19_181019.tdp21` TDP2.1 output

The wake trajectory and circulation decay output is written in non-dimensional form if **`nondim_output`** is set to **`true`** in the namelist file. The vortex locations (y, z) for both port and starboard vortices (**`Yp`**, **`Zp`**, **`Ys`**, and **`Ys`**) are normalized by the initial vortex pair separation (b_0) specified in the ADATA file for that case,

$$y^* = y / b_0 ; \quad z^* = z / b_0 \tag{1}$$

The circulation values in the time history, Γ for both port and starboard vortices (**`Gs`** and **`Gp`**) are normalized by the initial circulation strength Γ_0,

$$\Gamma^* = \Gamma / \Gamma_0 \tag{2}$$

Γ_0 is calculated using the values of initial vortex pair descent velocity, V_0 and the initial vortex pair separation, b_0 from the ADATA file

$$\Gamma_0 = 2\pi V_0 b_0 \tag{3}$$

The non-dimensional time, t^* is given by

$$t^* = t / t_0 \tag{4}$$

where $t_0 = b_0 / V_0$ is the time taken by the vortex pair to descend a distance equal to b_0.

In addition to the model output, for each run the environmental initial conditions are also written to files for plotting purposes if **`env_profiles`** is set to **`true`** in the namelist file.

`2003_09_19_181019.uplt`	Crosswinds
`2003_09_19_181019.vplt`	Headwinds
`2003_09_19_181019.qplt`	EDR
`2003_09_19_181019.tplt`	Theta/Temperature

Model Output File Example (e.g., YYYY_MO_DY_HRMNSC.apa38)

The model output file is written in the Tecplot® format. First three lines in the file contain header information, followed by the wake vortex track. An example of the output file is shown below.

MODEL OUTPUT (YYYY_MO_DY_HRMNSC.apa38)

```
TITLE="APA 3.8"
VARIABLES = "Time(s)", "Yp(m)", "Zp(m)", "Gp(m^2/s)", "Ys(m)", "Zs(m)", "Gs(m^2/s)"
ZONE T="31", I= 1097
   0.000     8.356    41.821    63.793    25.164    41.821    63.793
   0.100     8.300    41.761    63.738    25.108    41.761    63.738
   0.200     8.243    41.700    63.683    25.051    41.700    63.683
   0.300     8.187    41.640    63.627    24.995    41.640    63.627
   0.400     8.130    41.580    63.572    24.938    41.580    63.572
   0.500     8.074    41.520    63.517    24.882    41.520    63.517
   0.600     8.017    41.460    63.461    24.825    41.460    63.461
   0.700     7.960    41.399    63.406    24.768    41.399    63.406
   0.800     7.904    41.339    63.351    24.712    41.339    63.351
   0.900     7.847    41.279    63.296    24.655    41.279    63.296
   1.000     7.790    41.220    63.241    24.598    41.220    63.241
   1.100     7.734    41.160    63.186    24.542    41.160    63.186
   1.200     7.677    41.100    63.131    24.485    41.100    63.131
   1.300     7.620    41.040    63.076    24.428    41.040    63.076
   1.400     7.563    40.980    63.021    24.371    40.980    63.021
   1.500     7.507    40.921    62.966    24.315    40.921    62.966
   1.600     7.450    40.861    62.912    24.258    40.861    62.912
   1.700     7.393    40.802    62.857    24.201    40.802    62.857
   1.800     7.336    40.742    62.802    24.144    40.742    62.802
   1.900     7.279    40.683    62.748    24.087    40.683    62.748
   2.000     7.222    40.623    62.693    24.030    40.623    62.693
   and so on.....
```

Memphis Wake Vortex Field Experiment (1995)

A comprehensive field experiment to measure wake vortices and the associated ambient meteorological conditions was conducted at the Memphis International Airport in Memphis, Tennessee from August 6 through August 29, 1995 (Zak 1995; Campbell, et al. 1997). The experiment was sponsored under NASA Langley Research Center's Aircraft Vortex Spacing System (AVOSS) project (Hinton 1995; Perry et al. 1997). The wake data were collected using a continuous wave Lidar (Figure 1). The meteorological sensors included radiosondes, sodars, a wind profiler, one 150ft high meteorological tower, a Radio Acoustic Sounding System (RASS), and NASA Langley's OV-10 research aircraft. The radiosondes were used to measure winds and temperature measurements (10s averages) at 50m vertical resolution. The OV-10 aircraft was flown at selected times and took measurements of temperature and winds at a sample rate of 10Hz. Temperature (5min averages) was measured using RASS every 30min at 14 vertical levels from 127m to 1492m. The 150ft (45.7m) meteorological tower was equipped with a large array of sensor systems. Winds, temperature, and moisture were measured from the tower at 5m, 10m, 20m, 30m, and 42m heights. Turbulence quantities (turbulence kinetic energy and eddy dissipation rate) were estimated from wind measurements at 5m and 40m heights. Rain rate, soil temperature, soil moisture, barometric pressure, and incoming and outgoing solar radiation also were measured by the sensors deployed on the meteorological tower. Standard meteorological data such as atmospheric pressure, temperature, moisture, cloud cover, visibility, etc. were obtained from the National Weather Service's Surface Aerodrome Observations (SAO) and the Automated Surface Observations System (ASOS).

Data Processed for Fast-Time Wake Models

Eddy Dissipation Rate

EDR profiles were estimated using the two sonic anemometers on the meteorological tower and extrapolating to heights using atmospheric boundary layer similarity theory. The profiles were generated using the atmospheric turbulence profile generator (ATPG) code which implements the algorithms described in Han et al. (2000). Turbulence profiles were extrapolated to the ground ($z = 0$) and to a height above the observed vortices with a constant EDR value whenever the measured profiles did not extend to those heights.

Stratification

Temperature profiles were estimated using a fusion of the RASS and temperature sensors on the ASOS and the meteorological tower. The temperature profiles were converted to potential temperatures using the dry adiabatic lapse rate. The highest temperature measurement on the tower was at approximately 43m AGL and the lowest observation of the RASS was at 127m. A known deficiency in the profiles is a frequent mismatch in these two temperatures, leading to unrealistic gradients in the temperature profile within this region. This can sometimes lead to highly unstable persistent regions that are not attached to the ground. The potential temperature profiles were therefore pre-processed to remove these unstable regions by making the potential temperature constant in these regions.

Crosswinds and Headwinds

The profiles of the mean crosswind and headwind were generated by the AVOSS Winds Analysis System (AWAS) using an optimal estimation of data fusion from several different wind sensors including two Doppler radars, the meteorological tower, and the SODAR. There are some known deficiencies in the AWAS profiles which are discussed in detail by Dasey et al. (1998). In the current distribution, crosswinds and headwinds are included.

The coordinate system used in the input files is aircraft centric. The port/starboard vortex is always associated with the port/starboard side of the aircraft. In Figure 2 winds from west to east are shown. The crosswinds will be considered positive for landings and negative for departures even though the actual wind direction is same for both cases.

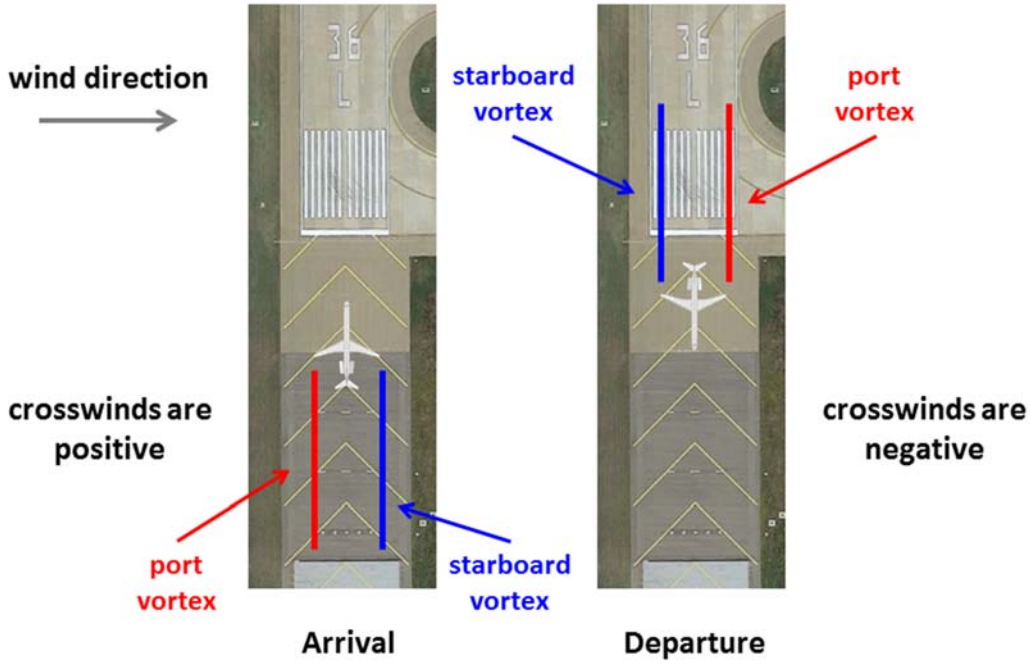

Figure 2: The coordinate system used in the input files is aircraft centric. The port/starboard vortex is always associated with the port/starboard side of the aircraft. In the figure the crosswinds are considered positive for landings and negative for takeoffs, even though the crosswinds are from the west to east in both cases.

Aircraft Data

The aircraft data used by the fast-time wake prediction models include the initial position (offset) of the vortex pair with respect to the runway centerline (y_0), the initial height of the vortices (z_0), the initial vortex descent rate (V_0) and the initial separation of vortices (b_0).

The initial position (offset) of the vortex pair with respect to the runway centerline y_0 was estimated using an average of the first few data points for each landing. The initial height of the vortices z_0 was estimated from backward extrapolation of the altitude trajectory in time. The initial separation distance between the vortices b_0 was estimated assuming an elliptical wing loading,

$$b_0 = \frac{\pi}{4} b_G \tag{3}$$

where b_G is the wingspan of the aircraft. The initial vortex descent rate was estimated from the aircraft weight, aircraft speed, air density, and the initial vortex separation b_0,

$$V_0 = \frac{W_G}{2\pi \rho V_G b_0^2} \tag{4}$$

where ρ is the air density - which was assumed to be 1.2kg/m^3 for all the landings at Memphis, V_G is the reported airspeed, and W_G is the reported landing weight of the aircraft.

Types of aircraft observed at different measurement sites are listed in Table 2 and a graphical presentation of aircraft distribution is shown in Figures 3-4. The Armory site was located south of the airport, while the TANG, Tchulahoma, and Threshold sites were all located at the north end of the airport.

Table 2: Aircraft Observed at different Measurement Sites

Aircraft Type	Armory	TANG	Tchulahoma	Threshold	Total
AT42	1	1	-	-	2
B727	86	1	3	24	114
B737	3	-	-	-	3
B757	5	2	1	-	8
BA31	-	-	2	-	2
DC10	25	-	-	2	27
DC9	57	19	6	3	85
EA30	11	-	-	-	11
EA31	9	-	-	1	10
EA32	15	7	2	1	25
FK10	5	2	-	-	7
MD11	-	-	-	1	1
SF34	2	-	8	-	10
Total	**219**	**32**	**22**	**32**	**305**

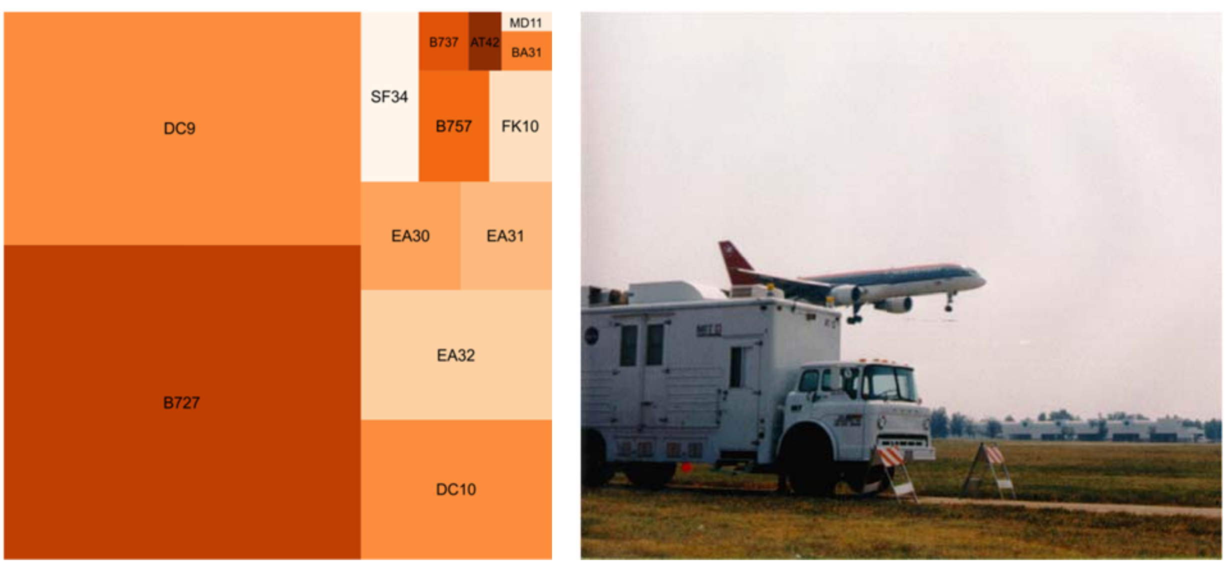

Figure 3: Distribution of the aircraft types in the Memphis 1995 dataset is shown in the left panel. A B757 landing in the background of the NASA Lidar van is shown in the right panel.

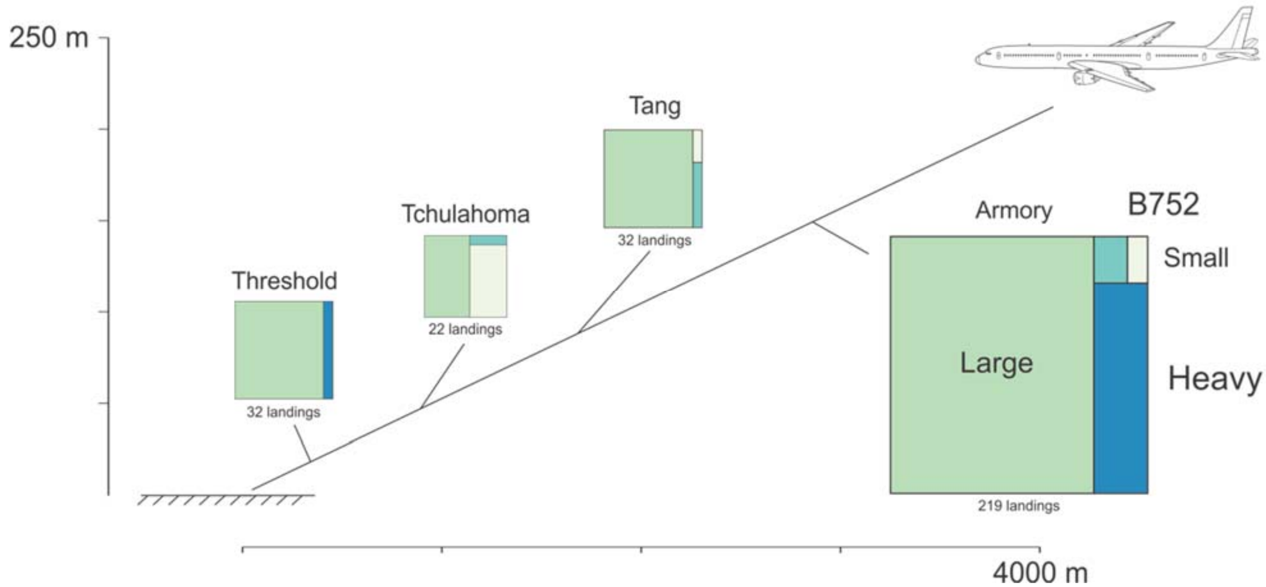

Figure 4: Distribution of the Lidar data by aircraft category and location. The Armory site was located south of the airport, while the TANG, Tchulahoma, and Threshold sites were all located at the north end of the airport.

Dallas/Fort Worth Wake Vortex Field Experiment (1997)

The deployment at the Dallas/Fort Worth International Airport in 1997 (Dasey et al. 1998; Joseph et al. 1999) was sponsored under NASA Langley Research Center's Aircraft Vortex Spacing System (AVOSS) project (Hinton 1995). Wake measurements were obtained from NASA's 2µm pulsed Lidar, the Lincoln Lab's 10.6µm Continuous Wave Lidar and an array of anemometers (windline). One of the objectives was to collect meteorological data for the validation of mesoscale models and therefore an impressive array of meteorological sensors was deployed to quantify the atmospheric state in detail. Two meteorological towers were installed during this field experiment. Each meteorological tower was equipped with various sensor systems for the measurement of temperature, relative humidity, wind speed, and wind direction at different heights. Turbulence measurements were taken with sonic anemometers which measured the three components of wind at 10Hz. Several sensors were mounted at the base of each tower to measure the atmospheric pressure, rainfall, and solar radiation, etc. In addition to the two meteorological towers, a wind profiler, a Radio Acoustic Sounding System (RASS) and a SOnic Detection And Ranging (SODAR) sensor were also deployed. Special upper air soundings were taken six times a day from five different sites surrounding the Dallas-Fort Worth International Airport. Standard meteorological data such as atmospheric pressure, temperature, moisture, cloud cover, and visibility were obtained from the National Weather Service's Surface Aerodrome Observations (SAO) and the Automated Surface Observations System (ASOS) data. The raw data in the Dallas/Fort Worth dataset have been processed to generate initial conditions for fast-time wake models. There are a total of 208 cases in this dataset that are provided with this distribution.

The aircraft, crosswinds, headwinds, turbulence, and stratification data from the Dallas/Fort Worth deployment were processed in the same manner as described for Memphis.

Denver Wake Vortex Field Experiment (2003)

The Denver field experiment was conducted by NASA during late August and September 2003. Although the primary objective for this deployment was to evaluate wake measurements using acoustic sensors (Dougherty et al. 2004), wake trajectories and circulation were also measured using pulsed and continuous wave Lidars. In addition, temperature profiles were measured with the MTP5 sensor (microwave radiometer), and wind profiles from the pulsed Lidar measurements. During the Denver experiment, one minute average winds were measured by propeller anemometers that were mounted on a meteorological tower. The altitudes of the sensors were at 7m, 14.6m, and 32.3m AGL. In addition, wind measurements at a rate of 10Hz were obtained with an ultrasonic anemometer that was mounted on a 7.3m pole. The generation of a vertical profile of eddy dissipation rate requires two data points at different heights (Han 2000). In the Denver 2003 experiment there was only one sonic anemometer, therefore the profiles of eddy dissipation rates were obtained from the Lidar data using spatial structure functions (Pruis et al. 2013). The initial conditions for fast-time wake models obtained from this dataset are included in this distribution.

Data Processed for Fast-Time Wake Models

Eddy Dissipation Rate

For the Denver 2003 dataset, the EDR profiles were estimated directly from the pulsed Doppler Lidar data. To calculate EDR profiles from the Lidar data, azimuthal structure function estimates were used to estimate the parameters of the turbulent wind field after correcting for the spatial averaging of the lidar pulse and the contribution from the estimation error of the velocity estimates (Pruis et al. 2013; Pruis and Delisi, 2011).

The structure function for a Gaussian transmitted Lidar pulse assuming a von Kármán model for the turbulent wind field (Frelich et al., 1998) is

$$D_{wgt}(s,\sigma,L_o) = 2\sigma^2 G(s/\Delta p, \Delta p/\Delta r, (2\ln 2)^{1/2}\Delta p/\Delta r), \tag{5}$$

where G is given by Eq. (46) in Frelich et al. (2006), s is the spacing between velocity estimates, σ^2 is the variance of the velocity, L_o is the outer scale of turbulence, Δp is the range gate length and Δr is the full pulse width at half maximum. When the estimation error is uncorrelated with the pulse-weighted velocity estimate an unbiased estimate for the velocity structure function of the mean Doppler Lidar velocity estimates is

$$\hat{D}_{wgt}(s) = \hat{D}_{raw}(s) - E(s) \tag{6}$$

where

$$\hat{D}_{raw}(k\Delta s) = \frac{1}{(N_T - k)} \sum_{j=1}^{N_T - k} \{\hat{v}'[(j-1)\Delta s] - \hat{v}'[(j+k-1)\Delta s]\}^2 \tag{7}$$

is the raw estimate of the azimuthal velocity structure function, and N_T is the number of velocity estimate bins for a given height interval.

This is analogous to the focused continuous wave Lidar technique described by Banakh et al. (1999) and later extended to pulsed Lidar measurements (Smalikho et al., 2005; Banakh et al., 2010). It assumes Tayler's frozen turbulence hypothesis is valid. To estimate the unbiased correction $E(s)$ for the contribution from the velocity estimation error for the separation distance kΔs we used the covariance technique described in Frehlich and Cornman (2001), where $E(k\Delta s)=2\sigma e(k\Delta s)$ because the velocity estimation error is uncorrelated with the pulse-weighted velocity and each estimate is produced with different Lidar pulses (Frehlich et al., 2006).

The azimuthal structure functions are computed by binning the pulsed Lidar horizontal in-plane velocity estimates in both height and azimuthal distance. For this analysis, a 13.5m bin size was used in both directions. Since the spatial structure functions may vary substantially from scan to scan due to the stochastic nature of turbulence, fifteen minutes of averaging was done for each estimate.

The parameters of the wind field σ and L_0 are then estimated by minimizing the χ^2 between the structure function estimates and the model predictions; that is

$$\chi^2 = \frac{1}{N_T}\sum_{k=1}^{N_T}\frac{[\hat{D}_{wgt}(k\Delta s) - D_{wgt}(k\Delta s,\sigma,L_0)]^2}{D_{wgt}^2(k\Delta s,\sigma,L_0)}. \tag{8}$$

If the azimuthal separation distance is small compared to the outer scale of turbulence ($s << L_0$) and the turbulence is isotropic, then the energy dissipation rate can be estimated (Kolmogorov, 1890; Monin and Yaglom, 1975) for each height bin as

$$\varepsilon = 0.933668\frac{\sigma^3}{L_0}, \tag{9}$$

assuming the Kolmogorov constant $C_v = 2$.

Vertical profiles of the eddy dissipation rate for individual landings were then estimated using the nearest neighbor EDR profiles estimated using the results estimated from the spatial structure functions. Figure 5 shows EDR profiles using the structure function for September 19th, 2003.

Stratification

Temperature profiles were obtained with a MTP-5 temperature profiler. The MTP-5 profiler estimates temperature at 50m increments and during the experiment profiles were nominally generated every five minutes. Profiles were smoothed in time using a 30-minute boxcar filter, and the measured temperature was converted to a potential temperature profile assuming a dry adiabatic lapse rate of 0.00976 degrees per meter.

Crosswinds and Headwinds

The profiles of the mean crosswind were generated for each track using the average of the CTI WindTracer® wind profile taken before and after each wake measurement and written in the track data files. Headwind profiles were not calculated for this data set.

Aircraft Data

The aircraft data generated for use in the fast-time wake prediction models at Denver was processed in the same manner as described for Memphis.

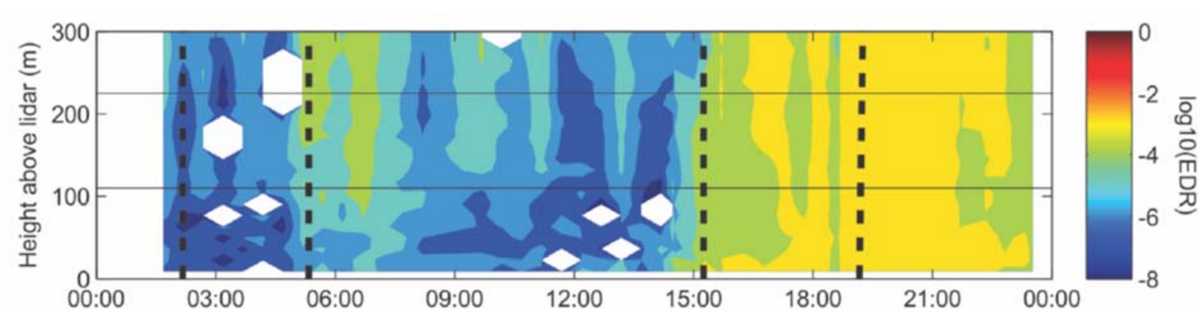

Figure 5: Eddy dissipation rate estimated from Lidar data using spatial structure functions every 30 minutes on September 19th, 2003 (Pruis et al. 2013). Times shown are UTC. Local time is UTC – 6 hours.

Evaluation of Fast-Time Models

Several evaluations of NASA's fast-time models have been conducted in the past (Proctor 2009; Pruis and Delisi 2011a; Feigh et al. 2012). Under a NASA Research Announcement, the NorthWest Research Associates (NWRA) was tasked to conduct an independent evaluation of NASA's fast-time models over a three year period. This evaluation concluded that, in general, the model circulation predictions had a mean root mean square error on the order of $0.2\Gamma_0$ to $0.3\Gamma_0$ (Γ_0 is the initial wake circulation), the vertical transport errors were on the order of $0.5b_0$, and the lateral transport errors were on the order of b_0 (Pruis and Delisi 2011a). NWRA also demonstrated that the lateral transport errors can be reduced to as low as $0.5b_0$ if more accurate crosswind initial conditions (e.g., by using proxy crosswinds as initial conditions) were provided to the fast-time models (Pruis et al. 2011). In this section the current distribution of the fast-time models are evaluated using the continuous wave Lidar observations from the Memphis 1995 field experiment, the Dallas/Fort Worth 1997 field experiment, and the Denver 2003 wake vortex data.

For the Memphis data, the groupings of the landings were based on the measurement site where the observations were obtained. The OGE observations are the measurements obtained at the 36R_Armory site, where the mean initial vortex height was 180m (all heights are AGL). The NGE observations were obtained from the 18L_TANG site where the mean initial observations, were at a height of 99m. The IGE data came from two different Lidar locations; the 27_Tchulahoma and the 27_Threshold data. The mean height of the initial vortex observation for these two sites was 36m.

The Dallas/Fort Worth data was collected with the Lincoln Laboratory 10.6µm Continuous-Wave (CW) Lidar. The NGE data was collected for arrivals on runway 17C with a vortex generation height of approximately 80 to 110 meters height above the ground. The NGE data were collected over 4 days during which the wind speeds varied between 5 and 20knots. The DFW IGE data were also collected with the Lincoln Laboratory CW Lidar. The data were collected over two days for aircraft on approach to runway 35C. The vortex generation height for these data was between 10 and 30 meters and the wind speeds ranged from light and variable up to 9 knots.

The Denver 2003 data were collected in the OGE phase. The data were collected with a CTI (Coherent Technologies Incorporated) WindTracer® pulsed Doppler Lidar. The data were collected for aircraft on approach to runway 16L. The vortex generation height was approximately 220 meters above ground. The Denver data set was collected over a one month time interval (late August and September) and covers a large range of atmospheric conditions.

The accuracy of predictions for the two models was quantified in terms of root mean square error (rmse), mean absolute error (mae), and bias. The prediction errors in TDP2.1, and APA3.8 for all Memphis 1995 cases are given in Table 3. The errors in TDP2.1 and APA3.8 categorized approximately by phase (OGE and NGE/IGE) are given in Tables 4-5. Proxy crosswinds were not used in this evaluation. Model prediction errors for the Dallas/Fort Worth 1997 and Denver 2003 are given in Tables 6 and 7 respectively.

Table 3: Memphis 1995: All 305 Cases

Model	Circulation (normalized by Γ_0)			Lateral Transport (normalized by b_0)			Altitude (normalized by b_0)		
	rmse	mae	bias	rmse	mae	bias	rmse	mae	bias
TDP21	0.263	0.224	0.028	1.01	0.832	0.095	0.528	0.45	0.072
APA38	0.251	0.215	-0.037	1.029	0.854	0.222	0.559	0.480	0.16

Table 4: Memphis 1995 (OGE): 219 Cases

Model	**Circulation (normalized by Γ_0)**			**Lateral Transport (normalized by b_0)**			**Altitude (normalized by b_0)**		
	rmse	**mae**	**bias**	**rmse**	**mae**	**bias**	**rmse**	**mae**	**bias**
TDP21	0.254	0.218	0.037	1.061	0.871	0.166	0.588	0.5	0.065
APA38	0.239	0.205	-0.022	1.091	0.904	0.337	0.63	0.542	0.204

Table 5: Memphis 1995 (NGE and IGE): 86 Cases

Model	**Circulation (normalized by Γ_0)**			**Lateral Transport (normalized by b_0)**			**Altitude (normalized by b_0)**		
	rmse	**mae**	**bias**	**rmse**	**mae**	**bias**	**rmse**	**mae**	**bias**
TDP21	0.288	0.242	0	0.85	0.712	-0.132	0.34	0.29	0.093
APA38	0.291	0.247	-0.088	0.832	0.696	-0.147	0.336	0.287	0.015

Table 6: Dallas/Fort Worth 1997 (NGE and IGE): 208 Cases

Model	**Circulation (normalized by Γ_0)**			**Lateral Transport (normalized by b_0)**			**Altitude (normalized by b_0)**		
	rmse	**mae**	**bias**	**rmse**	**mae**	**bias**	**rmse**	**mae**	**bias**
TDP21	0.289	0.242	-0.002	0.643	0.519	-0.215	0.29	0.241	0.047
APA38	0.287	0.241	-0.088	0.597	0.493	-0.089	0.287	0.24	-0.06

Table 7: Denver 2003 (OGE): 775 Cases

Model	**Circulation (normalized by Γ_0)**			**Lateral Transport (normalized by b_0)**			**Altitude (normalized by b_0)**		
	rmse	**mae**	**bias**	**rmse**	**mae**	**bias**	**rmse**	**mae**	**bias**
TDP21	0.306	0.285	0.244	1.301	1.198	0.111	0.657	0.554	-0.054
APA38	0.242	0.222	0.196	1.304	1.2	0.119	0.663	0.560	0.074

Generation of Initial Conditions for Applications

Pre- and post-processing of the input and output data is required for custom applications. Users can generate vertical profiles of environmental conditions for their applications using either sensor data or numerical weather prediction models. The current software design of the fast-time models assumes operations in the terminal area. For example, the initial lateral position of the vortex pair (y_0) is treated as an offset with respect to the runway centerline. If the models are used with flight data then appropriate coordinate transformations are required. Two application examples are briefly described in this section.

Ahmad et al. (2014) evaluated the wake models using wake encounter flight test data (Figure 6). The crosswind, stratification, and eddy dissipation rate were estimated from the data collected by sensors on the aircraft (Vicroy et al. 1998). Two sets of deterministic simulations were performed. In the first set, an instance of fast-time models was initialized every second along the C-130 trajectory, using the y_0, z_0, V_0 and crosswinds at that location (Figure 6). In the second set of simulations, averaged values of V_0 and crosswinds along the entire trajectory were used. Coordinate transformations were required to convert the fast-time output of wake location to latitude-longitude-altitude space for visualization and analysis purposes.

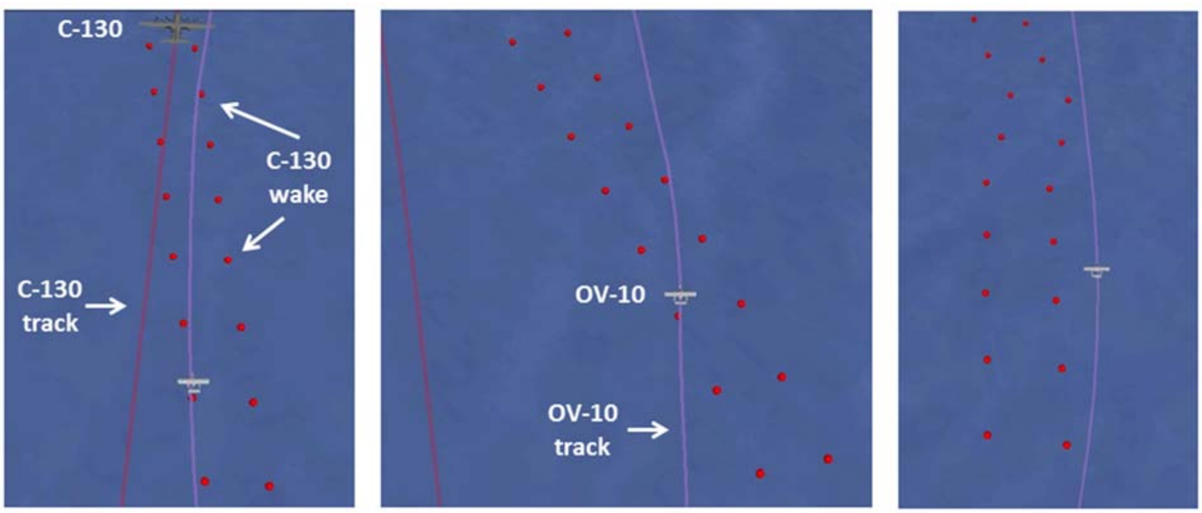

Figure 6: Simulations of NASA's wake vortex encounter flight test. C-130 was the wake generator and the OV-10 was the follower aircraft. An instance of TDP2.1 was initialized every second in the simulation shown in the figure (Ahmad et al. 2014).

The second example demonstrates the application of the fast-time models for safety analysis and accident investigations. A Cessna Citation aircraft crashed at the Will Rogers World Airport in Oklahoma City, Oklahoma on December 21, 2012. The NTSB carried out an investigation of this accident and concluded that the accident was likely due to a wake vortex encounter (O'Callaghan, 2013). To determine the likelihood of a wake vortex encounter, NTSB investigation data was used to evaluate the fast-time wake vortex models. The wake models in these simulations were used in the probabilistic mode (Gloudemans et al. 2016). The input data for this analysis was obtained from the NTSB report and included trajectories and aircraft parameters for the wake generator and the follower as well as detailed weather data. Publicly available data from the airport surveillance radar and the Cessna's onboard Enhanced Ground Proximity Warning System (EGPWS) provided both aircraft's latitude, longitude, and altitude, and the Cessna's orientation and airspeed.

Figure 7 shows the creation, evolution, and the advection of the simulated wake vortex bounds with the crosswinds. The red boxes indicate the area where the wake vortex centers are expected within the 2σ-bounds. The results of this analysis agreed with the NTSB report's estimated vortex location and indicated the possibility of an inadvertent vortex encounter preceding the Cessna's un-commanded roll.

Figure 7: The A300 and its track are shown in the figure along with the APA3.4 predicted vortex bounds. The Cessna encountering the wake bounds predicted by the model is also shown in the figure (Gloudemans et al. 2016).

APA Subroutine Calling Arguments

In addition to the inputs described in previous sections, the models use several other parameters. The default values of these parameters are hard-coded in the driver routine. These parameters and their default values are given in Table 8. Parameters which are read from input files are identified in the Default column of Table 8 and the output parameters list the output filename in the Default column of Table 8. The user needs to provide the parameters/data read in from the input files. Other parameters initialized in the main driver should not be changed. The calling arguments for TDP2.1 and APA3.8 are described in detail in this section. Default values for previous versions of APA model are also provided in Table 8.

TDP Version 2.1

The following call is made from the driver to the TDP2.1 routine:

```
      call APATDP(YZA, ZZA, VZA, BZA, ZMFA, ZGFA, GMFA, GRFA, GNGA,
     X            NTA, TZA, TA, NUA, UZA, UA, NQA, QZA, QA,
     X            AT1, AT2, NTOGA, AT1IM, AT2IM, NTIMGA,
     X            AT1GE1, AT2GE1, NTGE1A, AT1GE2, AT2GE2, NTGE2A,
     X            KMAXA, ADTFAC, AEPS, AH1, AHMIN,
     X            NB, TB, YPB, ZPB, GPB, YSB, ZSB, GSB, FLAG)
```

APA Version 3.8

The following call is made from the driver to the APA3.8 routine:

```
      call APA38(YZA, ZZA, VZA, BZA, ZMFA, ZGFA, GMFA, GRFA, GNGA,
     X           NTA, TZA, TA, NUA, UZA, UA, NHA, HZA, HA, NQA, QZA, QA,
     X           AT1, AT2, NTOGA, AT1IM, AT2IM, NTIMGA,
     X           AT1GE1, AT2GE1, NTGE1A, AT1GE2, AT2GE2, NTGE2A,
     X           KMAXA, ADTFAC, AEPS, AH1, AHMIN,
     X           ADOGE, ADIMG, ADGE1, ADGE2, ADFAC, ASPEED, AGLDANG,
     X           NB, TB, YPB, ZPB, GPB, YSB, ZSB, GSB, FLAG)
```

Table 8: Description of Calling Arguments

#	Parameter	Description	Defaults			
			TDP2.1	APA3.2	APA3.4	APA3.8
1	YZA	Initial lateral position of the vortex (units in MKS)	Read from *.ADATA			
2	ZZA	Initial altitude of the vortex (units in MKS)	Read from *.ADATA			
3	VZA	Initial descent speed of the vortex, V_0 (units in MKS)	Read from *.ADATA			
4	BZA	Initial separation between the vortex pair, b_0 (units in MKS)	Read from *.ADATA			
5	ZMFA	ZMFA*BZA is the altitude at which Phase II begins	1.25	1.5	1.5	1.5
6	ZGFA	ZGFA*BZA is the altitude at which Phase III begins	0.6	0.6	0.6	0.6
7	GMFA	GMFA is the ratio of the circulation of the ground effect vortices to the circulation of the primary vortices at the time they enter ground effect	0.25	0.4	0.35	0.3 (or 0.18 when over trees) Read from *.ADATA (only used by APA3.8)
8	GRFA	GRFA*BZA is the initial distance of the ground effect vortices from the primary vortices at the time they enter ground effect	0.4	0.4	0.4	0.4
9	GNGA	GNGA is the absolute value of the initial angle to the vertical made by the line between the primary and ground effect vortices. This angle is counterclockwise (clockwise) for the port (starboard) vortices	0	45.0	45.0	45.0
10	NTA	Number of points in temperature profile (should be 3 or more, and extend above and below heights of vortex prediction) negative value implies potential temperature (°K) positive value implies temperature (°K)	Read from *.TDATA			
11	TZA	Altitude corresponding to the temperature values (m)	Read from *.TDATA			
12	TA	Temperature or Potential Temperature values (°K)	Read from *.TDATA			
13	NUA	Number of points in crosswind profile (should be 3 or more, and extend above and below heights of vortex prediction)	Read from *.UDATA			
14	UZA	Altitude corresponding to the crosswind values (m)	Read from *.UDATA			
15	UA	Crosswind values (m/s)	Read from *.UDATA			
16	NQA	Number of points in eddy dissipation rate (EDR) profile (should be 3 or more, and extend above and below heights of vortex prediction)	Read from *.QDATA			
17	QZA	Altitude corresponding to the EDR values (m)	Read from *.QDATA			
18	QA	Eddy dissipation rate (EDR) values (m^2/s^3)	Read from *.QDATA			
19	AT1	Start time for Phase I	0	0	0	0
20	AT2	End time for Phase I	360	360	360	360

#	Parameter	Description	Defaults			
			TDP2.1	APA3.2	APA3.4	APA3.8
21	NTOGA	Number of time points for Phase I. If NTOGA < 0, then as the evolution proceeds, if circulation goes to zero, the lateral positions of the vortices at the time this occurs are maintained as time increases. If NTOGA > 0, then the vortices are allowed to advect with the wind. Since vortices with zero circulation essentially cease to exist, NTOGA is usually defined as < 0. Once read in, NTOGA is redefined as ABS(NTOGA).	-3601	-3601	-3601	-3601
22	AT1IM	Start time for Phase II	0	0	0	0
23	AT2IM	End time for Phase II	360	360	360	360
24	NTIMGA	Number of time points for Phase II (negative value indicates use of crosswind shear gradient term, positive value will run TDP without the crosswind shear gradient term)	-361	-361	-361	-361
25	AT1GE1	Start time for Phase III	0	0	0	0
26	AT2GE1	End time for Phase III	360	360	360	360
27	NTGE1A	Number of time points for Phase III	361	361	361	361
28	AT1GE2	Start time for Phase IV	0	0	0	0
29	AT2GE2	End time for Phase IV	360	360	360	360
30	NTGE2A	Number of time points for phase IV	361	361	361	361
31	KMAXA	Parameter used by the ODE solver routines	20000	20000	20000	20000
32	ADTFAC	Parameter used by the ODE solver routines	0.01	0.01	0.01	0.01
33	EPSA	Parameter used by the ODE solver routines	1.0E-6	1.0E-6	1.0E-6	1.0E-6
34	AH1	Parameter used by the ODE solver routines	0.01	0.01	0.01	0.01
35	AHMIN	Parameter used by the ODE solver routines	1.0E-10	1.0E-10	1.0E-10	1.0E-10
36	ADOGE	Used in the calculation of circulation decay rate (Phase I)	9999.	9999.	9999.	9999.
37	ADIMG	Used in the calculation of circulation decay rate (Phase II)	9999.	8	9999.	9999.
38	ADGE1	Used in the calculation of circulation decay rate (Phase III)	35	6	12	12
39	ADGE2	Used in the calculation of circulation decay rate (Phase IV)	35	6	12	12
40	ADFAC	Determines the decay rate due to EDR	9999.	0.55	0.4	0.4

#	Parameter	Description	Defaults			
			TDP2.1	APA3.2	APA3.4	APA3.8
41	NB	Model output: number of time history data points	Written to model output file			
42	TB	Model output: time (s)	Written to model output file			
43	YPB	Model output: lateral position of port vortex (m)	Written to model output file			
44	ZPB	Model output: altitude of port vortex (m)	Written to model output file			
45	GPB	Model output: circulation strength of port vortex (m^2/s)	Written to model output file			
46	YSB	Model output: lateral position of starboard vortex (m)	Written to model output file			
47	ZSB	Model output: altitude of starboard vortex (m)	Written to model output file			
48	GSB	Model output: circulation strength of starboard vortex (m^2/s)	Written to model output file			
49	FLAG	Error flag	N/A	N/A	N/A	N/A
50	cwshi	Factor used to determine amount of effect crosswind has on the upwind/downwind vortex in IGE, increases linearly from 0 to CWFHI as CW* increases from 0 to CWSHI	N/A	N/A	N/A	1.5
51	cwfhi	Factor used to modify the strength of the upwind/downwind secondary vorticity in IGE, i.e., GMFA*(1 +/- cwfhi)	N/A	N/A	N/A	0.5
52	facnge	Factor to modify strength of measured crosswind in the Near Ground Effect region	N/A	N/A	N/A	1.0
53	facige	Factor to modify strength of measured crosswind in the In Ground Effect region	N/A	N/A	N/A	1.0
54	NHA	Number of points in headwind profile (should be 3 or more, and extend above and below heights of vortex prediction)	Read from *.VDATA (only used by APA3.8)			
55	HZA	Altitude corresponding to the headwind values (m)	Read from *.VDATA (only used by APA3.8)			
56	HA	Headwind values (m/s)	Read from *.VDATA (only used by APA3.8)			
57	gslope	Glide slope (degree)	Read from *.ADATA (only used by APA3.8)			
58	ACspeed	Airspeed (m/s)	Read from *.ADATA (only used by APA3.8)			

Code Development and Evaluation

George Greene developed one of the earliest versions of fast-time wake vortex prediction models at NASA in the 1980s. The primary developers of the APA model are George Greene, Donald Delisi, Turgut Sarpkaya, Robert Robins, and Fred Proctor. The TDP model was developed by Fred Proctor, David Hamilton, and George Switzer. In addition, the following have contributed in the development and or evaluation of the wake models (in alphabetical order): Nashat Ahmad, Donald Bagwell, Fanny Limon Duparcmeur, David Hinton, Ed Johnson, David Lai, Matthew Pruis, David Rutishauser, and Randal VanValkenburg.

Bibliography

Ahmad, NN, MJ Pruis, "Evaluation of Fast-Time Wake Models using Denver 2006 Field Experiment Data," American Institute of Aeronautics and Astronautics, AIAA Paper 2015-3318.

Ahmad, NN, RL VanValkenburg, RL Bowles, FM Limon Duparcmeur, T Gloudemans, S van Lochem, E Ras, "Evaluation of Fast-Time Wake Vortex Models using Wake Encounter Flight Test Data", American Institute of Aeronautics and Astronautics, AIAA Paper 2014-2466.

Ahmad, NN, FH Proctor, FM Limon Duparcmeur, D Jacob, "Review of Idealized Aircraft Wake Vortex Models", American Institute of Aeronautics and Astronautics, AIAA Paper 2014-0927.

Ahmad, NN, FH Proctor, RL VanValkenburg, MJ Pruis, FM Limon Duparcmeur, "Mesoscale Simulation Data for Initializing Fast-Time Wake Transport and Decay Models", American Institute of Aeronautics and Astronautics, AIAA Paper 2013-0510.

Ahmad, NN, FH Proctor, "Estimation of Eddy Dissipation Rates from Mesoscale Model Simulations", American Institute of Aeronautics and Astronautics, AIAA Paper 2012-0429.

Banakh, VA, IN Smalikho, EL Pichugina, WA Brewer, "Representativeness of measurements of the dissipation rate of turbulence energy by scanning Doppler lidar," *Atmospheric and Oceanic Optics*, Vol. 23, 2010, pp. 48-54.

Banakh, VA, IN Smalikho, F Köpp, C Werner, "Measurements of Turbulent Energy Dissipation Rate with a CW Doppler Lidar in the Atmospheric Boundary Layer," *Journal of Atmospheric and Oceanic Technology*, Vol. 16, 1999.

Barmore, BE, NN Ahmad, MC Underwood, "Advanced Interval Management (IM) Concepts of Operations," National Aeronautics and Space Administration, 2014, NASA/TM-2014-218664.

Campbell, SD, et al., "Wake Vortex Field Measurement Program at Memphis, TN Data Guide", Lincoln Laboratory, Massachusetts Institute of Technology. Project Report NASA/L-2. 1997.

Charney, JJ, ML Kaplan, Y Lin, KD Pfeiffer, "A New Eddy Dissipation Rate Formulation for the Terminal Area PBL Prediction System (TAPPS)", American Institute of Aeronautics and Astronautics, AIAA Paper 2000-0624.

Corjon, A, T Poinsot, "Behavior of Wake Vortices Near Ground," *AIAA Journal*, Vol. 35, 1997, pp. 849-855.

Corjon, A, T Poinsot, "Vortex Model to Define Safe Aircraft Separation Distances," *Journal of Aircraft*, Vol. 33, 1996, pp. 547-553.

Dasey, TJ, RE Cole, RM Heinrichs, MP Matthew, GH Perras, "Aircraft Vortex Spacing System (AVOSS) Initial 1997 System Deployment at Dallas/Ft. Worth (DFW) Airport," Lincoln Laboratory, Massachusetts Institute of Technology, Project Report NASA/L-3, 1998.

Delisi, DP, RE Robins, MJ Pruis, "APA 3.8 Fast-Time, Numerical Wake Model Description and First Results", American Institute of Aeronautics and Astronautics, AIAA Paper 2016-3437.

Delisi, DP, MJ Pruis, D Jacob, DY Lai, "First Results from the NASA Wake Vortex Measurements at the Memphis International Airport", American Institute of Aeronautics and Astronautics, AIAA Paper 2014-2467.

Delisi, DP, MJ Pruis, F Wang, DY Lai, "Estimates of the Initial Vortex Separation Distance, bo, of Commercial Aircraft from Pulsed Lidar Data," American Institute of Aeronautics and Astronautics, AIAA Paper 2013-365.

Delisi, DP, RE Robins, GF Switzer, DY Lai, FY Wang, "Comparison of Numerical Model Simulations and SFO Wake Vortex Windline Measurements," American Institute of Aeronautics and Astronautics, AIAA Paper 2003-3810.

Delisi, DP, RE Robins, “Short-scale Instabilities in Trailing Wake Vortices in a Stratified Fluid,” *AIAA Journal*, Vol. 38, 2000, pp. 1916-1923.

De Visscher, I, et al., “Fast Time Modeling of Ground Effects on Wake Vortex Transport and Decay“, *Journal of Aircraft*, Vol. 50, 2013, pp. 1514-1525.

De Visscher, I, et al., “Aircraft Vortices in Stably Stratified and Weakly Turbulent Atmospheres: Simulation and Modeling“, *Journal of Aircraft*, Vol. 51, 2013, pp. 551-566.

De Visscher, I, G Winckelmans, T Lonfils, L Bricteux, M Duponcheel, N Bourgeois, "The Wake4D simulation platform for predicting aircraft wake vortex transport and decay: Description and examples of application", American Institute of Aeronautics and Astronautics, AIAA Paper 2010-7994.

Dougherty, RP, FY Wang, ER Booth, ME Watts, N Fenichel, RE D’Errico, “Aircraft Wake Vortex Measurements at Denver International Airport,” American Institute of Aeronautics and Astronautics, AIAA Paper 2004-2880.

Feigh, KM, L Sankar, V Manivannan, “Statistical Determination of Vertical Resolution Requirements for Real-Time Wake-Vortex Prediction”, *Journal of Aircraft*, Vol. 49, 2012, pp. 822-835.

Frech, M, F Holzäpfel, A Tafferner, T Gerz, “High-Resolution Weather Database for the Terminal Area of Frankfurt Airport”, *Comptes Rendus Physique*, Vol. 6, 2005, pp. 501-523.

Frehlich, R, Y Meillier, ML Jensen, B Balsley, R. Sharman, “Measurements of Boundary Layer Profiles in an Urban Environment,” *Journal of Applied Meteorology and Climatology*, Vol. 45, 2006, pp. 821-837.

Frehlich, R, SM Hannon, SW Henderson, “Coherent doppler lidar measurements of wind field statistics,” *Boundary-Layer Meteorology*, Vol. 86, 1998, pp. 233-256.

Frehlich, R, L Cornman, “Estimating Spatial Velocity Statistics with Coherent Doppler Lidar,” *Journal of Atmospheric and Oceanic Technology*, 2001, pp. 355-356.

Gerz, T, F Holzäpfel, D Darracq, “Commercial aircraft wake vortices”, *Progress in Aerospace Sciences*, Vol. 38, 2002, pp. 181-208.

Gerz, T, F Holzäpfel, W Gerling, A Scharnweber, M Frech, K Kober, K Dengler, S Rahm, "The Wake Vortex Prediction and Monitoring System WSVBS Part II: Performance and ATC Integration at Frankfurt Airport", *Air Traffic Control Quarterly* Vol. 17, 2009, pp. 323-346.

Gerz, T, F Holzäpfel, W Bryant, F Köpp, M Frech, A Tafferner, G Winckelmans, “Research towards a wake vortex advisory for optimal aircraft spacing”, *Journal of Applied Meteorology and Climatology*, Vol. 46, 2007, pp. 1913-1932.

Greene, GC, “An Approximate Model of Vortex Decay in the Atmosphere”, *Journal of Aircraft*, Vol. 23, 1986, pp. 566-573.

Gloudemans, T, S van Lochem, E Ras, J Malissa, NN Ahmad, TA Lewis, 2016: A Coupled Probabilistic Wake Vortex and Aircraft Response Prediction Model. National Aeronautics and Space Administration. NASA/TM-2016-219193.

Guerreiro, NM, KW Neitzke, SC Johnson, HP Stough, BT McKissick, HI Syed, “Characterizing a Wake-free Safe Zone for the Simplified Aircraft-based Paired Approach Concept”, American Institute of Aeronautics and Astronautics, AIAA Paper 2010-7681.

Han, J, SP Arya, S Shen, Y Lin, “An Estimation of Turbulent Kinetic Energy and Energy Dissipation Rate Based on Atmospheric Boundary Layer Similarity Theory”, National Aeronautics and Space Administration, 2000, NASA/CR-2000-210298.

Han J, Y Lin, SP Arya, FH Proctor, “Numerical Study of Wake Vortex Decay and Descent in Homogeneous Atmospheric Turbulence,” *AIAA Journal*, Vol. 38, 2000, pp. 643-656.

Han, J, Y Lin, DG Schowalter, SP Arya, FH Proctor, “Large Eddy Simulation of Aircraft Wake Vortices within Homogeneous Turbulence: Crow Instability,” *AIAA Journal*, Vol. 38, 2000, pp. 292-300.

Hinton, DA, “Description of Selected Algorithms and Implementation Details of a Concept-Demonstration Aircraft Vortex Spacing System (AVOSS),” National Aeronautics and Space Administration, 2001, NASA/TM-2001-211027.

Hinton, DA, CR Tatnall, “A Candidate Wake Vortex Strength Definition for Application to the NASA Aircraft Vortex Spacing System (AVOSS),” National Aeronautics and Space Administration, 1997, NASA/TM-1997-110343.

Hinton, DA, “An Aircraft Vortex Spacing System (AVOSS) For Dynamical Wake Vortex Spacing Criteria”, Advisory Group for Aerospace Research and Development, North Atlantic Treaty Organization (NATO), 1996, AGARD-CP-584.

Hinton, DA, “Aircraft Vortex Spacing System (AVOSS) Conceptual Design”, National Aeronautics and Space Administration, 1995, NASA/TM-1995-110184.

Holzäpfel, F, N Tchipev, A Stephan, “Wind Impact on Single Vortices and Counter-Rotating Vortex Pairs in Ground Proximity”, American Institute of Aeronautics and Astronautics, AIAA Paper 2015-3174.

Holzäpfel, F, “Effects of Environmental and Aircraft Parameters on Wake Vortex Behavior”, *Journal of Aircraft*, Vol. 51, 2014, pp. 1490-1500.

Holzäpfel, F, K Dengler, T Gerz, C Schwarz, “Prediction of Dynamic Pairwise Wake Vortex Separations for Approach and Landing”, American Institute of Aeronautics and Astronautics, AIAA Paper 2011-3037.

Holzäpfel, F, T Gerz, C Schwarz, "The Wake Vortex Prediction and Monitoring System WSVBS, Design and Performance at Frankfurt and Munich Airport”, *Proceedings of the 9th USA/Europe Air Traffic Management Research and Development Seminar* (ATM2011), 2011.

Holzäpfel, F, T Misaka, I Hennemann, “Wake-Vortex Topology, Circulation, and Turbulent Exchange Processes”, American Institute of Aeronautics and Astronautics, AIAA Paper 2010-7992.

Holzäpfel, F, T Gerz, M Frech, A Tafferner, F Köpp, I Smalikho, S Rahm, K Hahn, C Schwarz, "The Wake Vortex Prediction and Monitoring System WSVBS Part I: Design". *Air Traffic Control Quarterly*, Vol. 17, 2009, pp. 302-322.

Holzäpfel, F, M Frech, T Gerz, A Tafferner, K Hahn, C Schwarz, H Joos, B Korn, H Lenz, R Luckner, G Höhne, "Aircraft wake vortex scenarios simulation package - WakeScene", *Aerospace Science and Technology*, Vol. 13, 2009, pp. 1-11.

Holzäpfel, F, M Steen, “Aircraft wake-vortex evolution in ground proximity: Analysis and parameterization.” *AIAA Journal*, Vol. 45, 2007, pp. 218–227.

Holzäpfel, F, “Probabilistic Two-Phase Aircraft Wake-Vortex Model: Further Development and Assessment”, *Journal of Aircraft*, Vol. 43, 2006, pp. 700-708.

Holzäpfel, F., “Probabilistic Two-Phase Wake-Vortex Decay and Transport Model,” *Journal of Aircraft*, Vol. 40, 2003, pp. 323-331.

Holzäpfel, F., T. Gerz, M. Frech, A. Dörnbrack, "Wake Vortices in Convective Boundary Layer and their Influence on Following Aircraft," *Journal of Aircraft*, Vol. 37, 2000, pp. 1001-1007.

Jacob, D, MJ Pruis, DY Lai, DP Delisi, “Assessment of WakeMod 4: A New Standalone Wake Vortex Algorithm for Estimating Circulation Strength and Position,” American Institute of Aeronautics and Astronautics, AIAA Paper 2015-3176.

Johnson, SC, GW Lohr, BT McKissick, TS Abbott, NM Guerreiro, P Volk, “Simplified Aircraft-Based Paired Approach: Concept Definition and Initial Analysis”, National Aeronautics and Space Administration, 2013, NASA/TP-2013-217994.

Joseph, R, T Dasey, R Heinrichs, “Vortex and Meteorological Measurements at Dallas/Ft. Worth Airport,” American Institute of Aeronautics and Astronautics, AIAA Paper 1999-0760.

Kaplan, ML, Y Lin, C J Ringley, ZG Brown, MT Kiefer, PS Suffern, AM Hoggarth, “Wake Vortex Environment Simulations from a Terminal Area PBL Prediction System (TAPPS)”, American Institute of Aeronautics and Astronautics, AIAA Paper 2006-1074.

Kaplan, ML, RP Weglarz, Y Lin, DB Ensley, JK Kehoe, D Decroix, “A Terminal Area PBL Prediction System for DFW”, American Institute of Aeronautics and Astronautics, AIAA Paper 1999-0983.

Kolmogorov, AN, “The local structure of turbulence in incompressible viscous fluid for very large Reynolds numbers,” *Royal Society, Proceeding, Series A Mathematical and Physical Sciences*, Vol. 434, 1890, pp. 9–13. Translation.

Köpp, F et al., “Comparison of wake-vortex parameters measured by pulsed and continuous-wave lidars.” *Journal of Aircraft*, Vol. 42, 2005, pp.916–923.

Körner, S, F Holzäpfel, "Multi-Model Ensemble Wake Vortex Prediction – Further Development and Probablistic Assessment", American Institute of Aeronautics and Astronautics, AIAA Paper 2016-3438.

Körner, S, F Holzäpfel, "Multi-model ensemble wake vortex prediction", *Aircraft Engineering and Aerospace Technology: An International Journal*, Vol. 88, 2016, pp. 331-340.

Körner, S, NN Ahmad, F Holzäpfel, RL VanValkenberg, "Multi-Model Ensemble Wake Vortex Prediction", American Institute of Aeronautics and Astronautics, AIAA Paper 2015-3173.

Lai, DY, Jacob, D, and Delisi, DP, “Assessment of Pulsed Lidar Measurements of Aircraft Wake Vortex Position Using a Lidar Simulator,” American Institute of Aeronautics and Astronautics, AIAA Paper 2010-7988.

Lang, S, J Tittsworth, W Bryant, P Wilson, C Lepadatu, D Delisi, D Lai, G Greene, "Progress on an ICAO Wake Turbulence Re-Categorization Effort", American Institute of Aeronautics and Astronautics, AIAA Paper 2010-7682.

MacCready, PB, “Standardization of Gustiness Values from Aircraft,” *Journal of Applied Meteorology*, Vol. 3, 1964, pp. 439-449.

Monin, AS, AM Yaglom, “Statistical Fluid Mechanics: Mechanics of Turbulence, Volume 2,” MIT Press, 1975, 874 pp.

O'Callaghan, J, "Aircraft Performance Wake Vortex Study", National Transportation Safety Board, NTSB ID: CEN13TA113, 2013.

O'Connor, CJ, DK Rutishauser, "Enhanced Airport Capacity Through Safe, Dynamic Reduction in Aircraft Separation: NASA's Aircraft VOrtex Spacing System (AVOSS)", National Aeronautics and Space Administration, 2001, NASA/TM-2001-211052.

Perry, RB, DA Hinton, RA Stuever, “NASA Wake Vortex Research for Aircraft Spacing,” American Institute of Aeronautics and Astronautics, AIAA Paper 1997-0057.

Proctor, FH, NN Ahmad, “Crosswind Shear Gradient Affect on Wake Vortices,” American Institute of Aeronautics and Astronautics, AIAA Paper 2011-3038.

Proctor, FH, NN Ahmad, G Switzer, F Limon Duparcmeur, “Three-Phased Wake Vortex Decay,” American Institute of Aeronautics and Astronautics, AIAA Paper 2010-7991.

Proctor, FH, “Interaction of Aircraft Wakes from Laterally Spaced Aircraft,” American Institute of Aeronautics and Astronautics, AIAA Paper 2009-343.

Proctor, FH, "Evaluation of Fast-Time Wake Vortex Prediction Models," American Institute of Aeronautics and Astronautics, AIAA Paper 2009-0344.

Proctor, FH, DW Hamilton, GF Switzer, "TASS Driven Algorithms for Wake Prediction," American Institute of Aeronautics and Astronautics, AIAA Paper 2006-1073.

Proctor, FH, DW Hamilton, DK Rutishauser, GF Switzer, 2004: Meteorology and Wake Vortex Influence on American Airlines FL-587 Accident. National Aeronautics and Space Administration. NASA/TM-2004-213018.

Proctor, FH, DW Hamilton, J Han, "Wake Vortex Transport and Decay in Ground Effect: Vortex Linking with the Ground," American Institute of Aeronautics and Astronautics, AIAA Paper 2000-0757.

Proctor, FH, "The NASA-Langley Wake Vortex Modelling Effort in Support of an Operational Aircraft Spacing System", American Institute of Aeronautics and Astronautics, AIAA Paper 1998-0589.

Proctor, FH, "Numerical Simulation of Wake Vortices Measured During the Idaho Falls and Memphis Field Programs", American Institute of Aeronautics and Astronautics, AIAA Paper 1996-2496.

Proctor, FH, "The Terminal Area Simulation System / Volume 1: Theoretical Formulation", National Aeronautics and Space Administration, 1987, NASA/CR-1987-4046.

Pruis, MJ, DP Delisi, D Jacob, D Lai, "Summary of NASA Wake and Weather Data Collection at Memphis International Airport: 2013-2015," American Institute of Aeronautics and Astronautics, AIAA Paper 2016-3274.

Pruis, MJ, DP Delisi, D Jacob, "Observations of Wake Vortices from Upward Looking Pulsed Doppler Lidar Data," American Institute of Aeronautics and Astronautics, AIAA Paper 2015-3177. 2015a.

Pruis, MJ, DP Delisi, D Jacob, "Effect of Atmospheric Sheets and Layers Near the Ground on Wake Vortex Transport and Decay," American Institute of Aeronautics and Astronautics, AIAA Paper 2015-3315. 2015b.

Pruis, MJ, DP Delisi, D Jacob, DY Lai, "Fast-time Wake Vortex Model Predictions Compared with Observations Behind Landing Aircraft Near the Ground," American Institute of Aeronautics and Astronautics, AIAA Paper 2015-3316. 2015c.

Pruis, MJ, DP Delisi, D Jacob, "Observations of Small-scale Atmospheric Variability and the Importance of Accurate Weather Information in Deterministic and Probabilistic Fast-time Wake Vortex," American Institute of Aeronautics and Astronautics, AIAA Paper 2014-2468.

Pruis, MJ, DP Delisi, NN Ahmad, FH Proctor, "Atmospheric Turbulence Estimates from a Pulsed Lidar," American Institute of Aeronautics and Astronautics, AIAA Paper 2013-0512.

Pruis, MJ, DP Delisi, "Observation Lifetime of an Aircraft Trailing Vortex Pair," American Institute of Aeronautics and Astronautics, AIAA Paper 2012-426.

Pruis, MJ, DP Delisi, "Assessment of Fast-Time Wake Vortex Prediction Models using Pulsed and Continuous Wave Lidar Observations at Several Different Airports," American Institute of Aeronautics and Astronautics, AIAA Paper 2011-3035. 2011a.

Pruis, MJ, DP Delisi, "Comparison of Ensemble Predictions of a New Probabilistic Fast-Time Wake Vortex Model and Lidar Observed Vortex Circulation Intensities and Trajectories," American Institute of Aeronautics and Astronautics, AIAA Paper 2011-3036. 2011b.

Pruis, MJ, DP Delisi, "Correlation of the Temporal Variability in the Crosswind and the Observation Lifetime of Vortices Measured with a Pulsed Lidar," American Institute of Aeronautics and Astronautics, AIAA Paper 2011-3199. 2011c.

Pruis, MJ, DP Delisi, NN Ahmad, "Comparisons of Crosswind Velocity Profile Estimates Used in Fast-Time Wake Vortex Prediction Models," American Institute of Aeronautics and Astronautics, AIAA Paper 2011-1002.

Ramsey, D, DP Chi Nguyen, “Characterizing Aircraft Wake Vortices with Ground-Based Pulsed Coherent Lidar: Effects of Vortex Circulation Strength and Lidar Signal-to-Noise Ratio on Spectral Signature”, American Institute of Aeronautics and Astronautics, AIAA Paper 2011-3198.

Ringley, CJ, Y Lin, ZG Brown, ML Kaplan, “The Development of a Boundary Layer Turbulence Database for Wake Vortex Applications”, American Institute of Aeronautics and Astronautics, AIAA Paper 2007-287.

Robins, RE, DP Delisi, GC Greene “Development and Validation of a Wake Vortex Predictor Algorithm,” American Institute of Aeronautics and Astronautics, AIAA Paper 1998-665.

Robins, RE, DP Delisi, “Further Development of a Wake Vortex Predictor Algorithm and Comparisons to Data,” American Institute of Aeronautics and Astronautics, AIAA Paper 1999-0757.

Robins, RE, DP Delisi, GC Greene, “Algorithm for Prediction of Trailing Vortex Evolution,” *Journal of Aircraft*, Vol. 38, 2001, pp. 911-917.

Robins, RE, DP Delisi, “NWRA AVOSS Wake Vortex Prediction Algorithm Version 3.1.1,” National Aeronautics and Space Administration, 2002, NASA/CR 2002-211746.

Robins, RE, DP Delisi, “Modeling Crosswind Shear Effects in NASA’s AVOSS Prediction Algorithm,” American Institute of Aeronautics and Astronautics, AIAA Paper 2006-1076.

Sarpkaya, T, “New Model for Vortex Decay in the Atmosphere,” *Journal of Aircraft*, Vol. 37, 2000, pp. 53-61.

Sarpkaya, T, RE Robins, and DP Delisi, “Wake-Vortex Eddy-Dissipation Model Predictions Compared with Observations,” *Journal of Aircraft*, Vol. 38, 2001, pp. 687- 692.

Smalikho, I, F Köpp, S Rahm, “Measurement of Atmospheric Turbulence by 2-μm Doppler Lidar, *Journal of Atmospheric and Oceanic Technology*, Vol. 22, 2005, pp. 1733-1747.

Sölch, I, F Holzäpfel, F Abdelmoula, D Vechtel, “Performance of Onboard Wake-Vortex Prediction Systems Employing Various Meteorological Data Sources,” *Journal of Aircraft*, Posted online on 29 Mar 2016.

Spalart, PR, “Airplane Trailing Vortices,” *Annual Review of Fluid Mechanics*, Vol. 30, 1998, pp. 107-138.

Vicroy, DD, PM Vijgen, HM Reimer, JL Gallegos, PR Spalart, “Recent NASA Wake-Vortex Flight Tests, Flow Physics Database and Wake-Development Analysis,” American Institute of Aeronautics and Astronautics, AIAA Paper 1998-5592.

Wing, DJ, WB Cotton, “For Spacious Skies: Self-Separation with “Autonomous Flight Rules” in US Domestic Airspace”, American Institute of Aeronautics and Astronautics, AIAA Paper 2011-6865.

Zak, JA, “Cases of Interesting Meteorological Conditions during Wake Vortex Measurements at Memphis, Tennessee during August 1995”, Vigyan Interim Report for NASA Contract NAS1-19341. 1996.

REPORT DOCUMENTATION PAGE	*Form Approved* *OMB No. 0704-0188*

1. REPORT DATE *(DD-MM-YYYY)*
01-11- 2016

2. REPORT TYPE
Technical Memorandum

3. DATES COVERED *(From - To)*

4. TITLE AND SUBTITLE
NASA AVOSS Fast-Time Models for Aircraft Wake Prediction: User's Guide (APA3.8 and TDP2.1)

5a. CONTRACT NUMBER

5b. GRANT NUMBER

5c. PROGRAM ELEMENT NUMBER

6. AUTHOR(S)
Ahmad, Nash'at N.; VanValkenburg, Randal L.; Pruis, Matthew J.; Limon Duparcmeur, Fanny M.

5d. PROJECT NUMBER

5e. TASK NUMBER

5f. WORK UNIT NUMBER
330693.04.20.07.03

7. PERFORMING ORGANIZATION NAME(S) AND ADDRESS(ES)
NASA Langley Research Center
Hampton, VA 23681-2199

8. PERFORMING ORGANIZATION REPORT NUMBER
L-20757

9. SPONSORING/MONITORING AGENCY NAME(S) AND ADDRESS(ES)
National Aeronautics and Space Administration
Washington, DC 20546-0001

10. SPONSOR/MONITOR'S ACRONYM(S)
NASA

11. SPONSOR/MONITOR'S REPORT NUMBER(S)
NASA-TM-2016-219353

12. DISTRIBUTION/AVAILABILITY STATEMENT
Unclassified - Unlimited
Subject Category 03
Availability: NASA STI Program (757) 864-9658

13. SUPPLEMENTARY NOTES

14. ABSTRACT
NASA's current distribution of fast-time wake vortex decay and transport models includes APA (Version 3.8) and TDP (Version 2.1). This User's Guide provides detailed information on the model inputs, file formats, and model outputs. A brief description of the Memphis 1995, Dallas/Fort Worth 1997, and the Denver 2003 wake vortex datasets is given along with the evaluation of models. A detailed bibliography is provided which includes publications on model development, wake field experiment descriptions, and applications of the fast-time wake vortex models.

15. SUBJECT TERMS
Aircraft wake turbulence; Wake vortex

16. SECURITY CLASSIFICATION OF: a. REPORT	b. ABSTRACT	c. THIS PAGE	17. LIMITATION OF ABSTRACT	18. NUMBER OF PAGES	19a. NAME OF RESPONSIBLE PERSON
					STI Help Desk (email: help@sti.nasa.gov)
U	U	U	UU	37	**19b. TELEPHONE NUMBER** *(Include area code)* (757) 864-9658

Standard Form 298 (Rev. 8/98)
Prescribed by ANSI Std. Z39.18